PHYSICAL REVIEW C **91**, 061301(R) (2015)

Infrared length scale and extrapolations for the no-core shell model

K. A. Wendt,[1,2] C. Forssén,[3,1,2] T. Papenbrock,[1,2] and D. Sääf[3]
[1]*Department of Physics and Astronomy, University of Tennessee, Knoxville, Tennessee 37996, USA*
[2]*Physics Division, Oak Ridge National Laboratory, Oak Ridge, Tennessee 37831, USA*
[3]*Department of Fundamental Physics, Chalmers University of Technology, SE-412 96 Göteborg, Sweden*
(Received 25 March 2015; published 3 June 2015)

We precisely determine the infrared (IR) length scale of the no-core shell model (NCSM). In the NCSM, the A-body Hilbert space is truncated by the total energy, and the IR length can be determined by equating the intrinsic kinetic energy of A nucleons in the NCSM space to that of A nucleons in a $3(A-1)$-dimensional hyper-radial well with a Dirichlet boundary condition for the hyper radius. We demonstrate that this procedure indeed yields a very precise IR length by performing large-scale NCSM calculations for ^{6}Li. We apply our result and perform accurate IR extrapolations for bound states of ^{4}He, ^{6}He, ^{6}Li, and ^{7}Li. We also attempt to extrapolate NCSM results for ^{10}B and ^{16}O with bare interactions from chiral effective field theory over tens of MeV.

DOI: 10.1103/PhysRevC.91.061301 PACS number(s): 21.60.De, 21.10.Dr, 03.65.Aa

Introduction. The spherical harmonic oscillator basis is a convenient and popular choice in nuclear structure calculations because it reflects the symmetries and the self-bound character of atomic nuclei. A finite oscillator space, defined by a maximum of N excited oscillator quanta and frequency ω, exhibits infrared (IR) and ultraviolet (UV) cutoffs π/L and Λ, respectively [1]. Here, $L \approx \sqrt{2N}b$ and $\Lambda \approx \sqrt{2N}/b$ (in units where $\hbar = 1 = c$) are leading-order (LO) approximations in N, valid for $N \gg 1$ [2,3], and $b \equiv \sqrt{\hbar/(M\omega)}$ denotes the oscillator length for a particle of mass M. This makes it necessary to understand the convergence of energies and other observables as L and Λ are increased. The UV convergence depends on the momentum regulators employed in the nuclear interaction [4], while the IR convergence depends on the structure of the nucleus under consideration. Coon *et al.* [5] found that the IR convergence of ground-state energies is exponential in L (in model spaces where corrections due to a finite UV cutoff Λ can be neglected). This exponential convergence can be understood as follows [6]: For long wavelengths, the finite oscillator basis is indistinguishable from a spherical well with a hard wall at a radius L, and the resulting Dirichlet boundary condition induces corresponding corrections to the exponential fall-off of bound-state wave functions. This insight allows one to derive IR extrapolation formulas for bound-state energies and radii [6,7].

For IR extrapolations to work in practice, one needs a value for the IR length L that is more precise than the LO result given in the previous paragraph. As it turns out, the next-to-leading order (NLO) value of L depends on the model space employed in the calculation, but the method to compute the IR length is system independent. For a single particle in $d = 3$ dimensions (or the deuteron in the center-of-mass system), More *et al.* [8] derived a very precise value of L by equating the lowest eigenvalue of the squared momentum operator in the finite oscillator basis with $(\pi/L)^2$, i.e., the lowest eigenvalue of the squared momentum operator in the infinite spherical well of radius L. The result (for a single particle in d dimensions) is

$$L = L_2(d) \equiv \sqrt{2(N + d/2 + 2)}b. \tag{1}$$

This result is NLO in N. While derived for a single-particle system, it has also been applied in extrapolations of nuclei with mass numbers $A > 2$; see, e.g., Refs. [9–12].

Very recently, Furnstahl *et al.* [13] derived a precise value of the IR length scale for A-fermion systems whose Hilbert space is a Cartesian product of single-particle oscillator spaces truncated at N. Such a Hilbert space is employed by several quantum many-body methods [9,14–20]. The key was again to equate the lowest eigenvalue of the total squared momentum operator in the finite oscillator basis to the lowest eigenvalue of the A-body kinetic energy in an infinite spherical well of radius L, keeping the exact dependence on N. The resulting IR length L differs in NLO from L_2, and numerical values are tabulated in Ref. [13].

We are still lacking a precise value of the IR length scale L for the many-body model space truncation employed in the no-core shell model (NCSM) [21,22]. This widely used method [23–29] employs a total energy truncation, i.e., a Hilbert space of all A-body product states with an energy not exceeding $N^{\rm tot}_{\rm max}\hbar\omega$. In the NCSM literature, the model space is usually specified by the number of excitations above the lowest configuration for the symmetry (parity, numbers of protons and neutrons) of interest. We denote this truncation by $N^{\rm NCSM}_{\rm max}$ in order to distinguish it from the total number of $\hbar\omega$ quanta, $N^{\rm tot}_{\rm max}$. The many-body character of this truncation implies that the total squared momentum operator is not a single-particle operator in this model space (and its eigenstates are not product states). Thus, the IR scale derived by Furnstahl *et al.* [13] is only a leading-order approximation of the many-body IR length scale. It is the purpose of this Rapid Communication to precisely determine the IR length scale of the NCSM.

We finally note that the convergence and corrections due to finite model spaces are also studied for interacting particles on lattices. Here, too, the effects of hard walls or periodic boundary conditions onto many-body bound states are of particular interest [30–35]. In contrast to the harmonic oscillator, the precise IR and UV cutoffs are easily identified on the lattice, and the effort goes into extrapolation formulas for relevant observables.

Infrared length scale of the NCSM. Let us consider $A = 3$ spinless fermions in $d = 1$ dimensions as an illustrative example. Following Refs. [7,8,13], we seek to equate the kinetic energy of this system in the NCSM space to the kinetic energy of a corresponding system in an infinite well of radius L. Our task consists of determining what the corresponding system really is. The Hilbert space is spanned by Slater determinants

$$\phi_{n_1 n_2 n_3}(x_1,x_2,x_3) = \det[\psi_{n_i}(x_j)]_{i,j=1,2,3} \tag{2}$$

of harmonic oscillator (HO) wave functions $\psi_n(x)$, and we only include three-body states that fulfill the total energy truncation

$$\sum_{i=1}^{A} n_i \leqslant N_{\max}^{\text{tot}} . \tag{3}$$

The key insight is that this Hilbert space of $A = 3$ particles in $d = 1$ dimensions is equivalent to that of a single particle in $Ad = 3$ dimensions, spanned by three-dimensional spherical harmonic oscillator wave functions

$$\phi_{nlm}(\mathbf{r}) = \phi_{nlm}(r,\theta,\varphi) = R_{nl}(r)Y_{lm}(\theta,\varphi) . \tag{4}$$

Here, R_{nl} is a radial wave function and Y_{lm} are spherical harmonics. The NCSM truncation of Eq. (3) is equivalent to allowing only those single-particle basis states ϕ_{nlm} with $2n + l \leqslant N_{\max}^{\text{tot}}$. However, we also need to consider the antisymmetry of the $A = 3$ wave function. If we align the projection axis of the spherical basis along the line $x_1 = x_2 = x_3$, antisymmetry can be obtained with wave functions proportional to $\sin 3\varphi$, i.e., m needs to be a multiple of three, which implies $l \geqslant 3$. Thus, with this additional symmetry constraint, the NCSM truncation for $A = 3$ particles in $d = 1$ dimensions naturally corresponds to a single particle in $Ad = 3$ dimensions, with single-particle energies limited to $N_{\max}^{\text{tot}}$. The IR properties of the single particle in a three-dimensional oscillator space are well known [8], and the harmonic oscillator truncation imposes a Dirichlet-like boundary condition on the radial coordinate.

As a check, we compute the eigenvalues of the kinetic energy for $A = 3$ fermions in $d = 1$ dimension (in a NCSM model space with $N_{\max}^{\text{tot}} = 80$) and compare them to the kinetic-energy spectrum of a three-dimensional hyper-radial well. The antisymmetry of the former system manifests itself as a discrete symmetry of the latter. The results are shown in Fig. 1 (middle and left spectrum, respectively) and also compared to the kinetic energy spectrum for three fermions in a one-dimensional infinite well (right spectrum). In each case, the entire spectrum is proportional to the inverse square of an underlying length scale, so we plot the eigenvalues T_i in units of the lowest kinetic energy eigenvalue T_0 to remove this dependence. Clearly the NCSM spectrum closely matches that of the hyper-radial well but not that of three particles in an infinite square well.

We can generalize these results as follows. The Hilbert space of A nucleons in $d = 3$ dimensions subject to the NCSM truncation identified by $N_{\max}^{\text{tot}}$ is equivalent to that of a single particle, with certain discrete symmetry constraints, in an Ad-dimensional HO space with single-particle energies up to $N_{\max}^{\text{tot}}$ excited quanta. At low momenta, the latter is

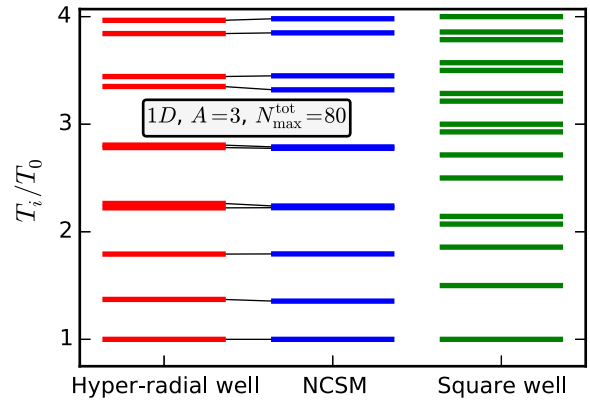

FIG. 1. (Color online) Comparison of kinetic energy spectra for three fermions in a hyper-radial well (left), three fermions in a one-dimensional NCSM basis (middle), and three fermions in a one-dimensional infinite square well (right).

equivalent to a hyper-radial well. Equating the kinetic energies yields the size of this well and consequently the IR length L of the corresponding NCSM basis. Alternatively, the NCSM truncation can also be viewed as a system of A fermions confined to an Ad dimensional hyper-radial well.

Let us therefore compute the eigenvalues of the kinetic energy for a D-dimensional hyper-radial well with an infinite wall at hyper radius L. The hyperspherical basis states can be labeled as $|\rho\, G\, \boldsymbol{\alpha}\rangle$, where ρ is the hyper radius, G is the grand angular momentum, and $\boldsymbol{\alpha}$ is the collection of all other partial-wave quantum numbers. The kinetic energy operator is block diagonal in both G and $\boldsymbol{\alpha}$, so we focus on a single arbitrary hyperspherical partial wave. The hyper-radial part of the noninteracting Hamiltonian is

$$-\left(\frac{\partial^2}{\partial\rho^2} - \frac{\mathcal{L}(\mathcal{L}+1)}{\rho^2}\right)\psi_G(\rho) = Q^2\psi_G(\rho) , \tag{5}$$

where $\mathcal{L} = G + (D-3)/2$ and Q^2 is the total squared momentum. The hyper-radial eigensolutions of this Hamiltonian are

$$\psi_G(\rho) = \sqrt{Q\rho}\, J_{\mathcal{L}+\frac{1}{2}}(Q\rho) , \tag{6}$$

where $J_\nu(X)$ is a Bessel function of the first kind. Imposing a Dirichlet boundary condition at $\rho = L$ implies that QL is a zero of $J_{\mathcal{L}+\frac{1}{2}}$. We denote the ith zero as $X_{i,\mathcal{L}}$. The selection criteria for $\mathcal{L}$ (yielding an antisymmetric wave function) is discussed below, but the entire spectrum of our well is now completely determined by a minimum value of $\mathcal{L}$ and the hyper radius L of the well

$$\left\{Q_{i,n}^2\right\} = \left\{L^{-2}X_{i,\mathcal{L}_{\min}+2n}^2\ \forall i,n \in \mathbb{Z}\right\}. \tag{7}$$

Here $\mathcal{L} = \mathcal{L}_{\min+2n}$ labels states of the same parity.

The next critical ingredient is the lowest eigenvalue of the kinetic energy operator in the NCSM basis. Recall that even though $\hat{T}$ is a one-body operator, the NCSM truncation

effectively promotes it to an A-body operator

$$\hat{T}_{\rm NCSM} = \left(\sum_{i=1}^{A} \hat{p}_i^2\right) \times \Theta\left(N_{\rm max}^{\rm tot}\hbar\omega - \sum_{i=1}^{A}\left(\frac{\hat{p}_i^2}{2M} + \frac{M\omega^2}{2}\hat{x}_i^2 - \frac{3}{2}\hbar\omega\right)\right). \tag{8}$$

Here Θ denotes the unit step function that enforces the NCSM truncation. Even though $\hat{T}_{\rm NCSM}$ is an A-body operator, the hyperspherical basis can be used to ease the computational requirement for finding its eigenvalues. Similar to the example discussed above, we can expand any product of three-dimensional HO states into hyper-radial harmonic oscillator states.

Likewise the transformation is block diagonal in the total oscillator quanta $\sum_{i=1}^{A}(2n_i + l_i) = 2N + G$, where N is the nodal quantum number for the hyper-radial coordinate. Exploiting this block diagonal structure, we need to only diagonalize small matrices, with dimension 5–20, instead of the full dimension of the NCSM basis. The kinetic energy matrix elements are

$$\langle NG\boldsymbol{\alpha}|\hat{T}_{\rm NCSM}|N'G'\boldsymbol{\alpha}'\rangle = \delta_G^{G'}\delta_{\boldsymbol{\alpha}}^{\boldsymbol{\alpha}'}\frac{\hbar\omega}{2}\left[\delta_N^{N'}\left(2N + \mathcal{L} + \frac{3}{2}\right) + \delta_{N_>}^{N_<+1}\sqrt{(N_< + 1)\left(N_< + \mathcal{L} + \frac{3}{2}\right)}\right], \tag{9}$$

and it will be sufficient to consider a single hyperspherical channel with grand angular momentum G. Here $N_< \equiv \min(N,N')$, $N_> \equiv \max(N,N')$, and N,N' run from 0 to $\lfloor\frac{N_{\rm max}^{\rm tot}-G}{2}\rfloor$, with the brackets $\lfloor . \rfloor$ denoting the integer part of their argument. We denote the needed dimensionless eigenvalues as $T_{i,\mathcal{L}}(N_{\rm max}^{\rm tot})$ such that

$$\hat{T}_{\rm NCSM}|i\rangle = \frac{\hbar\omega}{2}T_{i,\mathcal{L}}\left(N_{\rm max}^{\rm tot}\right)|i\rangle. \tag{10}$$

The smallest permitted eigenvalue is driven by the smallest symmetry-allowed value of $\mathcal{L} = G + (D-3)/2$. For a single-product state, $D = 3A$, and G can be decomposed as

$$G = \sum_{i=1}^{A} l_i + \sum_{i=1}^{A-1} n_{i,i+i}\,. \tag{11}$$

Here l_i is the orbital angular momentum and $n_{i,i+1}$ is the nodal quantum number for the hyperangle between the radial coordinates r_i and r_{i+1}, and A is the number of single-particle coordinates. In a single-particle basis, this means that the lowest possible value for G is $G_{\rm min,sp} = \sum_i l_{i,0}$, where $l_{i,0}$ are the orbital quantum numbers from the lowest (symmetry-allowed) energy configuration in the basis.

NCSM calculations for $A > 6$ usually employ single-particle coordinates (instead of relative coordinates [36,37]). However, the NCSM eigenstates are products of a center-of-mass state and an intrinsic state. Thus, the relevant IR length is an intrinsic scale. The dimension of the intrinsic basis is $D = 3(A-1)$, and $G_{\rm min}$ (the lowest value of the grand angular momentum in the relative coordinate system) is determined by the sum of intrinsic orbital angular momenta that can couple with spins to give the ground-state angular momentum J and parity Π. This means that $G_{\rm min} = G_{\rm min,sp}$ because the center-of-mass state carries no angular momentum.

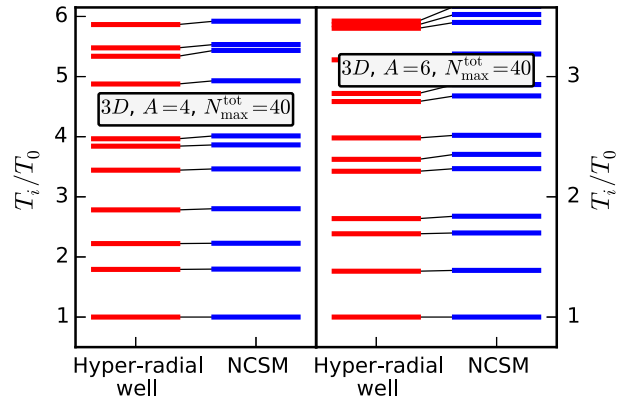

FIG. 2. (Color online) Discrete intrinsic kinetic energy spectra for $A = 4,6$ particles in the NCSM (right pane) and for the corresponding $D = 3(A-1)$ dimensional hyper-radial infinite well. In each case, we plot in units of the smallest eigenvalue.

The close similarity of the kinetic energy spectra of $3(A-1)$-dimensional hyper-radial wells with Dirichlet boundary condition and the corresponding intrinsic kinetic energies in a NCSM basis for $A = 4,6$ particles in three dimensions is shown in Fig. 2. For the large values of $N_{\rm max}^{\rm tot}$ employed in this numerical comparison, the agreement between the spectra persists up to highly excited states.

The intrinsic IR length is now obtained by equating the lowest kinetic energy eigenstate in the hyper-radial well, from Eq. (7), and the first eigenstate in the NCSM basis, from Eq. (10). This yields

$$L_{\rm eff} = b\frac{X_{1,\mathcal{L}}}{\sqrt{T_{1,\mathcal{L}}\left(N_{\rm max}^{\rm tot}\right)}} \tag{12}$$

with

$$\mathcal{L} = G_{\rm min} + \frac{3(A-2)}{2}. \tag{13}$$

Numerical values for $L_{\rm eff}$ are tabulated in the Supplemental Material [38].

Following König *et al.* [4] we exploit the duality of the HO Hamiltonian under the exchange of position and momentum operators and identify the UV scale of the NCSM as

$$\Lambda_{\rm eff} = \frac{X_{1,\mathcal{L}}}{b\sqrt{T_{1,\mathcal{L}}\left(N_{\rm max}^{\rm tot}\right)}} = L_{\rm eff}/b^2. \tag{14}$$

To illustrate that $L_{\rm eff}$ is indeed the correct IR scale of the NCSM basis we perform large-scale calculations of ^{6}Li for a wide range of HO frequencies $\hbar\omega$. We used the nucleon-nucleon interaction NNLO$_{\rm opt}$ [39] in model spaces up to $N_{\rm max}^{\rm NCSM} = 18$ ($N_{\rm max}^{\rm tot} = 20$). The UV-regulator cutoff of this interaction is 500 MeV. The model-space parameters

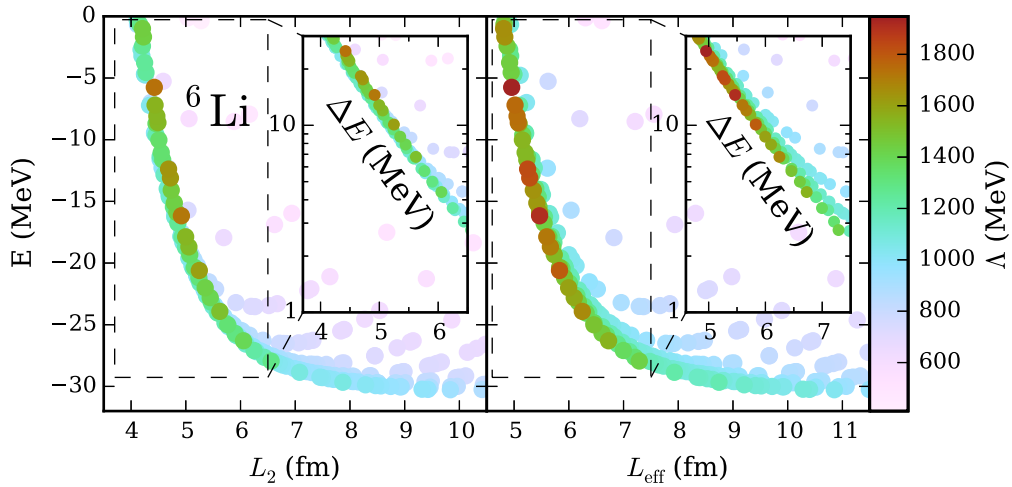

FIG. 3. (Color online) Ground-state energy of ^{6}Li plotted as a function of the IR scale determined by either L_2 [8] (left panel) or $L_{\rm eff}$ from this work (right panel). The color of each circular marker indicates the UV cutoff of that calculation, with darker colors corresponding to larger cutoffs. Insets show $\Delta E = E(L,\Lambda) - E_\infty$ on a semilogarithmic scale.

$(\hbar\omega, N_{\rm max}^{\rm NCSM})$ were converted to $(L_{\rm eff}, \Lambda_{\rm eff})$, using Eqs. (12) and (14).

The right panel of Fig. 3 shows that a common, exponential envelope is formed by the data with large UV cutoffs when plotted as a function of $L_{\rm eff}$. In particular, at a given value of $L_{\rm eff}$, the energy with the largest UV cutoff $\Lambda_{\rm eff}$ is lowest in energy. We also find that results from smaller model spaces deviate rather quickly from the IR envelope due to lack of UV convergence. The left panel of Fig. 3 shows the same energies plotted as a function of the IR scale L_2, with N in Eq. (1) corresponding to the highest single-particle state in the basis. While the points fall close to a line, no envelope is formed, and the data with the highest UV cutoff $\Lambda_2 = L_2/b^2$ is not lowest in energy at given L_2. The comparison of the left and right panels demonstrates that $L_{\rm eff}$ is a much more precise IR length for the NCSM than L_2, and this leads to more stable extrapolations.

Extrapolation results. The exponential IR extrapolations [5–7] can be generalized to the NCSM by employing the asymptotic wave function

$$\psi(\rho) \to e^{-\kappa\rho} - e^{-2\kappa L} e^{+\kappa\rho} \tag{15}$$

that is consistent with the Dirichlet boundary condition at hyper radius $\rho = L$. Here, κ denotes a hypermomentum. Asymptotically, i.e., for $\kappa L \to \infty$, the approximation (15) holds for any value of the grand angular momentum. For nonzero grand angular momentum, corrections to the coefficient $\exp(-2\kappa L)$ are of order $(\kappa L)^{-1}$, similar to corrections

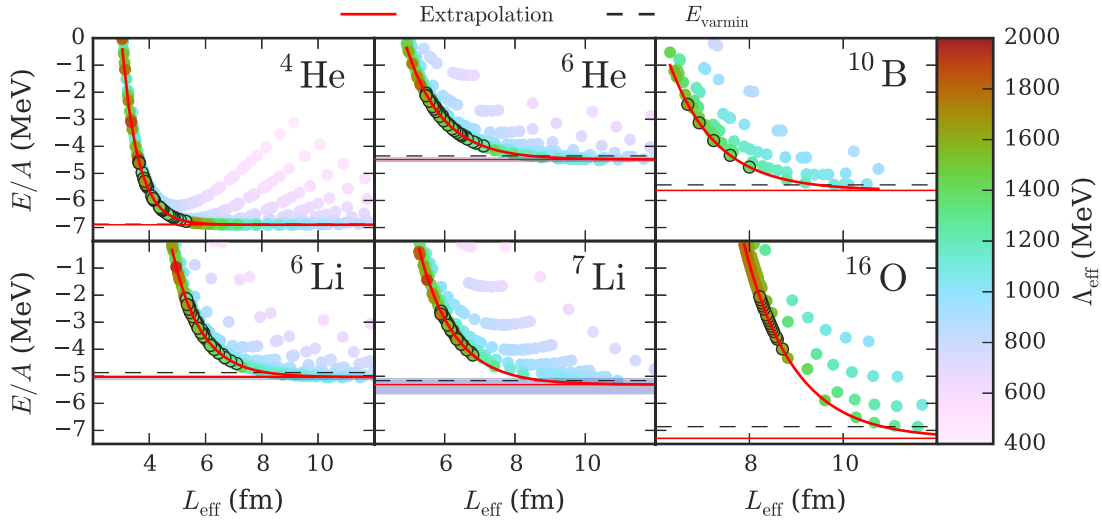

FIG. 4. (Color online) Extrapolations of the binding energy per particle for several p-shell nuclei computed with the NCSM. The color of each circular marker indicates the UV cutoff of that calculation with darker colors corresponding to larger cutoffs. Markers with a black border are included in the extrapolation. The solid red (gray) curve shows the exponential fit (16), and the horizontal red (gray) line marks the value of E_∞ with uncertainty estimates indicated as blue (gray) bands. The dashed black line marks the variational minimum $E_{\rm varmin}$ for the largest model space included in the fit.

due to finite angular momentum for a single particle in three dimensions [7]. Thus, we use a simple exponential form

$$E(L) = E_\infty + ae^{-2\kappa_\infty L}\,, \tag{16}$$

for IR extrapolations of bound-state energies. Here, the extrapolated energy E_∞ and the parameters a and κ_∞ will be fit to data points obtained in model spaces characterized by the IR length L. For the two-body system, a and κ_∞ are related to the asymptotic normalization coefficient and binding momentum, respectively [8].

In the NCSM the computational expense grows rapidly with increasing $N_{\max}^{\text{tot}}$. The IR extrapolation of a bound-state energy is useful if the resulting E_∞ (obtained from NCSM spaces with up to $N_{\max}^{\text{tot}}$) is closer to the exact result than the variational minimum energy that can be computed in a NCSM space with $N_{\max}^{\text{tot}}$. To locate the minimum, one needs at least three NCSM calculations. For IR extrapolations, one needs also at least three NCSM calculations, with parameters L_{eff} and Λ_{eff} such that (i) L_{eff} significantly exceeds the radius of the nucleus under consideration, (ii) Λ_{eff} significantly exceeds the UV cutoff of the interaction, and (iii) the resulting energies are negative.

Figure 4 shows extrapolations for the ground-state energies of ^{4}He, ^{6}He, ^{6}Li, ^{7}Li, ^{10}B, and ^{16}O. For the $A = 4,6$ systems we can perform NCSM calculations in very large model spaces for which the ground-state energies are virtually converged. However, in order to benchmark the effectiveness of the extrapolation we artificially restrict our data set to smaller models spaces, $N_{\max}^{\text{tot}} \leqslant 10$ and $N_{\max}^{\text{tot}} \leqslant 14$ respectively. For ^{7}Li, we use energies from model spaces with $N_{\max}^{\text{tot}} \leqslant 17$. The extrapolations for the nuclei ^{10}B and ^{16}O employ energies from a single model space of $N_{\max}^{\text{tot}} = 16$ and $N_{\max}^{\text{tot}} = 20$, respectively. Energies from smaller model spaces were not deemed sufficiently UV converged, as can be seen in the corresponding panels. For each nucleus, we select data with Λ_{eff} large enough that all points fall on a single narrow envelope and L_{eff} large enough that $E(L_{\text{eff}}) - E_\infty$ is exponential. The blue (gray) horizontal bands give an estimate of the uncertainly of the fit, obtained from refitting with all possible pairs of data excluded from the data set. Table I summarizes the results. The comparison to benchmark results shows that IR extrapolations are useful.

Summary. We determined the IR length scale of the NCSM by equating the intrinsic kinetic energy of A fermions subject to the NCSM truncation to the kinetic energy of A fermions in a $3(A-1)$ hyper-radial well with Dirichlet boundary condition for the single collective variable ρ. Calculations of ^{6}Li in large NCSM spaces show that the resulting IR length L_{eff} is correctly identified. We applied this result to extrapolate ground-state energies in ^{4,6}He, ^{6,7}Li, ^{10}B, and ^{16}O. The comparison with benchmark results shows that extrapolated energies are closer to the benchmarks than the minimum variational energies obtained in the model spaces utilized for the extrapolation. Further progress would depend on a better understanding of the extrapolation formula for the NCSM and in particular on combined UV and IR correction terms.

TABLE I. Energies (in MeV) of ground states with given spin and parity for several nuclei. Benchmark results E_{ref} from coupled-cluster calculations for ^{16}O [39] and from the NCSM for ^{4,6}He and ^{6}Li are obtained in large model spaces with $N_{\max}^{\text{tot}} = 20$ (equivalent to $N_{\max}^{\text{NCSM}} = 18$ for $A = 6$). Extrapolated energies E_∞ (with fit parameter κ_∞ in units of fm^{-1}) and variational minimum energies E_{varmin} are from smaller model spaces with $N_{\max}^{\text{tot}}$.

Nucleus	E_{ref}	E_{varmin}	E_∞	$N_{\max}^{\text{tot}}$	κ_∞
^{4}He(0^+)	−27.76	−27.51	−27.59	10	0.87
^{6}He(0^+)	−27.13	−26.12	−26.92	14	0.49
^{6}Li(1^+)	−30.27	−29.18	−30.17	14	0.49
^{7}Li($\frac{3}{2}^-$)	–	−36.11	−37.14	17	0.50
^{10}B(3^+)	–	−54.24	−56.29	16	0.50
^{16}O(0^+)	−130.1	−109.77	−116.75	20	0.47

Acknowledgments. We thank A. Ekström, R. J. Furnstahl, S. König, and P. Maris for useful discussions and H. T. Johansson and B. D. Carlsson for support with the large-scale NCSM calculations. This material is based upon work supported by the U.S. Department of Energy, Office of Science, Office of Nuclear Physics under Awards No. DEFG02-96ER40963 (University of Tennessee) and No. DE-SC0008499 (NUCLEI SciDAC Collaboration) and under Contract No. DE-AC05-00OR22725 (Oak Ridge National Laboratory). It was also supported by the Swedish Foundation for International Cooperation in Research and Higher Education (STINT, IG2012-5158) and by the European Research Council under the European Community's Seventh Framework Programme (FP7/2007-2013)/ERC Grant Agreement No. 240603.

[1] I. Stetcu, B. Barrett, and U. van Kolck, No-core shell model in an effective-field-theory framework, Phys. Lett. B **653**, 358 (2007).

[2] G. Hagen, T. Papenbrock, D. J. Dean, and M. Hjorth-Jensen, *Ab initio* coupled-cluster approach to nuclear structure with modern nucleon-nucleon interactions, Phys. Rev. C **82**, 034330 (2010).

[3] E. D. Jurgenson, P. Navrátil, and R. J. Furnstahl, Evolving nuclear many-body forces with the similarity renormalization group, Phys. Rev. C **83**, 034301 (2011).

[4] S. König, S. K. Bogner, R. J. Furnstahl, S. N. More, and T. Papenbrock, Ultraviolet extrapolations in finite oscillator bases, Phys. Rev. C **90**, 064007 (2014).

[5] S. A. Coon, M. I. Avetian, M. K. G. Kruse, U. van Kolck, P. Maris, and J. P. Vary, Convergence properties of *ab initio* calculations of light nuclei in a harmonic oscillator basis, Phys. Rev. C **86**, 054002 (2012).

[6] R. J. Furnstahl, G. Hagen, and T. Papenbrock, Corrections to nuclear energies and radii in finite oscillator spaces, Phys. Rev. C **86**, 031301 (2012).

[7] R. J. Furnstahl, S. N. More, and T. Papenbrock, Systematic expansion for infrared oscillator basis extrapolations, Phys. Rev. C **89**, 044301 (2014).

[8] S. N. More, A. Ekström, R. J. Furnstahl, G. Hagen, and T. Papenbrock, Universal properties of infrared oscillator basis extrapolations, Phys. Rev. C **87**, 044326 (2013).

[9] V. Somà, C. Barbieri, and T. Duguet, *Ab initio* Gorkov-Green's function calculations of open-shell nuclei, Phys. Rev. C **87**, 011303 (2013).

[10] E. D. Jurgenson, P. Maris, R. J. Furnstahl, P. Navrátil, W. E. Ormand, and J. P. Vary, Structure of *p*-shell nuclei using three-nucleon interactions evolved with the similarity renormalization group, Phys. Rev. C **87**, 054312 (2013).

[11] D. Sääf and C. Forssén, Microscopic description of translationally invariant core + N + N overlap functions, Phys. Rev. C **89**, 011303 (2014).

[12] R. Roth, A. Calci, J. Langhammer, and S. Binder, Evolved chiral NN + 3N Hamiltonians for *ab initio* nuclear structure calculations, Phys. Rev. C **90**, 024325 (2014).

[13] R. J. Furnstahl, G. Hagen, T. Papenbrock, and K. A. Wendt, Infrared extrapolations for atomic nuclei, J. Phys. G: Nucl. Part. Phys. **42**, 034032 (2015).

[14] W. Dickhoff and C. Barbieri, Self-consistent Green's function method for nuclei and nuclear matter, Prog. Part. Nucl. Phys. **52**, 377 (2004).

[15] D. J. Dean and M. Hjorth-Jensen, Coupled-cluster approach to nuclear physics, Phys. Rev. C **69**, 054320 (2004).

[16] G. Hagen, T. Papenbrock, D. J. Dean, and M. Hjorth-Jensen, Medium-mass nuclei from chiral nucleon-nucleon interactions, Phys. Rev. Lett. **101**, 092502 (2008).

[17] K. Tsukiyama, S. K. Bogner, and A. Schwenk, In-medium similarity renormalization group for nuclei, Phys. Rev. Lett. **106**, 222502 (2011).

[18] G. Hagen, T. Papenbrock, M. Hjorth-Jensen, and D. J. Dean, Coupled-cluster computations of atomic nuclei, Rep. Prog. Phys. **77**, 096302 (2014).

[19] H. Hergert, S. K. Bogner, S. Binder, A. Calci, J. Langhammer, R. Roth, and A. Schwenk, In-medium similarity renormalization group with chiral two- plus three-nucleon interactions, Phys. Rev. C **87**, 034307 (2013).

[20] S. Binder, J. Langhammer, A. Calci, and R. Roth, *Ab initio* path to heavy nuclei, Phys. Lett. B **736**, 119 (2014).

[21] P. Navrátil, S. Quaglioni, I. Stetcu, and B. R. Barrett, Recent developments in no-core shell-model calculations, J. Phys. G: Nucl. Part. Phys. **36**, 083101 (2009).

[22] B. R. Barrett, P. Navrátil, and J. P. Vary, *Ab initio* no core shell model, Prog. Part. Nucl. Phys. **69**, 131 (2013).

[23] P. Navrátil, J. P. Vary, and B. R. Barrett, Large-basis *ab initio* no-core shell model and its application to ^{12}C, Phys. Rev. C **62**, 054311 (2000).

[24] C. Forssén, P. Navrátil, W. E. Ormand, and E. Caurier, Large basis *ab initio* shell model investigation of ^{9}Be and ^{11}Be, Phys. Rev. C **71**, 044312 (2005).

[25] S. Quaglioni and P. Navrátil, *Ab initio* many-body calculations of n-^{3}H, n-^{4}He, p-^{3,4}He, and n-^{10}Be scattering, Phys. Rev. Lett. **101**, 092501 (2008).

[26] R. Roth and P. Navrátil, *Ab initio* Study of ^{40}Ca with an importance-truncated no-core shell model, Phys. Rev. Lett. **99**, 092501 (2007).

[27] T. Dytrych, K. D. Sviratcheva, J. P. Draayer, C. Bahri, and J. P. Vary, *Ab initio* symplectic no-core shell model, J. Phys. G: Nucl. Part. Phys. **35**, 123101 (2008).

[28] P. Maris, J. P. Vary, and A. M. Shirokov, *Ab initio* no-core full configuration calculations of light nuclei, Phys. Rev. C **79**, 014308 (2009).

[29] C. W. Johnson, W. E. Ormand, and P. G. Krastev, *Ab initio* symplectic no-core shell model, Comput. Phys. Commun. **184**, 2761 (2013).

[30] M. Lüscher, Volume dependence of the energy spectrum in massive quantum field theories, Commun. Math. Phys. **104**, 177 (1986).

[31] S. König, D. Lee, and H.-W. Hammer, Volume dependence of bound states with angular momentum, Phys. Rev. Lett. **107**, 112001 (2011).

[32] S. König, D. Lee, and H.-W. Hammer, Non-relativistic bound states in a finite volume, Ann. Phys. (NY) **327**, 1450 (2012).

[33] M. Pine and D. Lee, Effective field theory for bound state reflection, Ann. Phys. (NY) **331**, 24 (2013).

[34] R. Briceño, Z. Davoudi, and T. Luu, Two-nucleon systems in a finite volume: Quantization conditions, Phys. Rev. D **88**, 034502 (2013).

[35] R. A. Briceño, Z. Davoudi, T. C. Luu, and M. J. Savage, Two-nucleon systems in a finite volume. II. $^{3}S_{1} - {}^{3}D_{1}$ coupled channels and the deuteron, Phys. Rev. D **88**, 114507 (2013).

[36] N. Barnea and A. Novoselsky, Construction of hyperspherical functions symmetrized with respect to the orthogonal and the symmetric groups, Ann. Phys. (NY) **256**, 192 (1997).

[37] S. Bacca, M. A. Marchisio, N. Barnea, W. Leidemann, and G. Orlandini, Microscopic calculation of six-body inelastic reactions with complete final state interaction: Photoabsorption of ^{6}He and ^{6}Li, Phys. Rev. Lett. **89**, 052502 (2002).

[38] See Supplemental Material at http://link.aps.org/supplemental/10.1103/PhysRevC.91.061301 for a tabulation of numerical values for L_{eff}.

[39] A. Ekström, G. Baardsen, C. Forssén, G. Hagen, M. Hjorth-Jensen, G. R. Jansen, R. Machleidt, W. Nazarewicz, T. Papenbrock, J. Sarich, and S. M. Wild, Optimized chiral nucleon-nucleon interaction at next-to-next-to-leading order, Phys. Rev. Lett. **110**, 192502 (2013).